Interaction of CH$_4$ and H$_2$O in ice mixtures

Víctor J. Herrero, Óscar Gálvez,* Belén Maté and Rafael Escribano

Ice mixtures of methane and water are investigated by means of IR spectroscopy in the 14–60 K range. The spectroscopic research is focused on the symmetry-forbidden ν_1 band of CH$_4$ and the dangling bond bands of water. The ν_1 band is visible in the spectra of the mixtures, revealing a distorted methane structure which co-exists with the normal crystalline methane. The water dangling bond bands are found to increase their intensity and appear at red-shifted frequency when distorted methane is present. Methane adsorbed on water micropores or trapped inside the amorphous solid water structure is assumed to be responsible for these effects. CH$_4$ mobility in water ice depends on the deposition method used to prepare the samples and on the temperature. After warming the samples to 60 K, above the methane sublimation point, a fraction of CH$_4$ is retained in the water ice. An adsorption isotherm analysis is performed yielding the estimation of the desorption energy of CH$_4$ on H$_2$O amorphous surfaces.

1. Introduction

Icy systems composed of mixtures of frozen species are found in many different environments. On Earth, ice particles are constituents of clouds, where water can have other companions which often play fundamental atmospheric roles, like *e.g.* sulfuric acid in acid rain episodes, or nitric acid in polar stratospheric clouds. Snow-deposited ice usually contains gaseous species trapped inside, like CO$_2$, which is used to date geological strata in permanent ice regions like Antarctica or Greenland. Other planets and satellites of our Solar system have been shown to hold frozen amounts of different species.[1–4] The rocky core which constitutes comet nuclei is assumed to be surrounded by an icy layer, where water, CO, CO$_2$, CH$_4$ and CH$_3$OH are the main components. Further beyond, interstellar grains are also believed to be formed by a silicate or carbonaceous core covered by an icy mantle of light species, of which water is again usually the most abundant, hydrogen being assumed to have escaped or been recombined to produce other more stable species.

The CH$_4$/H$_2$O system is particularly interesting, from both astrophysical and geological points of view. It has been detected in comets and in interstellar grain mantles,[5–8] and the recent results of the Cassini-Huygens mission to Titan suggest the existence of methane clathrates under the surface of the satellite.[9–11] There is growing interest in a possible methane sequestration into, or release from, CH$_4$/H$_2$O mixtures, and, in general, in all possible kinds of association between these species, including clathrates, aerosols and in the solid state.[12–14]

Infrared spectroscopy is well suited to study these systems. The profile (shape, width, and peak position) of IR bands in the spectra of ice mixtures strongly depends on the structure of the ice and hence IR spectroscopy can reveal structural

Instituto de Estructura de la Materia, CSIC, Serrano 123, 28006 Madrid, Spain

information on the sample, often related to its generation method and thermal history. Laboratory experiments conducted on CH$_4$/H$_2$O samples reported changes in peak position, profiles and relative strength of IR bands with temperature and methane concentration.[15–20] There are also several studies on the morphology of water ices through CH$_4$ adsorption experiments.[21–23]

We present in this article an investigation on methane/water ice mixtures in the 14–60 K temperature range. The main tool used in this study is transmission IR spectroscopy. Following a description of the experimental method, the paper presents the main spectroscopic results, based on the observation of the dipole-forbidden breathing vibration of methane and the dangling bond bands of water, and the variation of these features with temperature and methane concentration. These spectroscopic findings are then discussed. In the following section, the desorption energy of methane from amorphous solid water (ASW) is estimated from isothermal adsorption experiments. The main conclusions are summarized at the end of the paper.

2. Experimental

All experiments were performed in a high vacuum chamber (base pressure in the 10^{-8} mbar range) described in detail before.[24,25] Ice films of H$_2$O, CH$_4$ and of mixtures of the two species were vapour-deposited on a cold silicon substrate cooled to 14 K by an ARS cryostat. The temperature of the substrate was measured with Si diodes and could be controlled, with 1 K accuracy, between 14 and 300 K by means of a Lakeshore temperature control module. H$_2$O vapour (distilled water, three times freeze-pump-thawed) and CH$_4$ (99.95%, Air Liquide) were admitted into the chamber through independent needle valves. The ice films were characterized by normal incident transmission spectroscopy at 2 cm^{-1} resolution (corresponding to *ca.* 0.5 cm mirror displacement in the interferometer), after co-adding 500 scans

for each spectrum. The spectra were recorded using a Bruker Vertex70 FTIR spectrometer purged with dry air. The system was provided with a differentially pumped quadrupole mass spectrometer (QMS) that allowed to check the purity of each species before deposition and to control the vapour stoichiometry during the deposition process.

The QMS was calibrated from measurements of the growth rate of solid films of the pure species.[26] By simulating our transmission spectra with the adequate optical constants taken from the literature, the film thicknesses needed for the calculation of the growth rate were derived. The typical thickness values ranged between 80 and 400 nm. For water ice grown at 14 K, we used the optical constants of Hudgins et al.[15] at 10 K. A sticking coefficient of 1 and a density of 0.7 g cm^{-3} were assumed at this temperature.[23,27] For CH$_4$ at 14 K, a sticking coefficient of 1 [28] and a density of 0.47 g cm^{-3} were used.[29] A mean value of the optical constants given by Hudgins et al.[15] for pure CH$_4$ at 10 and 20 K was used to simulate the IR spectra, because the CH$_4$ spectrum undergoes considerable changes over this temperature interval. The calibration of the QMS remained stable in the course of the present experiments as verified by periodic checks. The estimated error in the absolute pressure values was ~10%. Deposition pressures ranged between approximately 2×10^{-7} and 1×10^{-3} mbar.

Films of mixed CH$_4$/H$_2$O ices were prepared by sequential or simultaneous deposition of the vapours. In the first case, water ice was initially formed by depositing water vapour at 14, 40 or 50 K and then CH$_4$ vapour was added at specified temperatures. In the second scheme, H$_2$O and CH$_4$ were introduced into the chamber simultaneously, at the appropriate ratio, and allowed to deposit on the substrate, held at 14 or 40 K. To study the thermal behavior of the ices, the temperature was gradually raised at 10 K min^{-1}, and spectra were recorded at 30 and 60 K for ices deposited at 14 K, and at 60 K for ices deposited at 40 or 50 K.

The integrated values of the infrared absorption bands and the corresponding integrated absorption coefficients, A, were used to calculate the column densities of water and CH$_4$ in the ice mixtures via the following relation:

$$N = \frac{\text{Int}}{A} \qquad (1)$$

where N is the column density of absorbing molecules (the number of absorbers per unit area) in the beam and Int $= \int \ln(I_0/I)\mathrm{d}\nu$ is the integrated band peak area. The molecular ratio CH$_4$/H$_2$O in the mixtures is determined as the quotient of the respective column densities.

For this purpose the bands selected were the water OH-stretching band around 3.1 μm (3200 cm^{-1}) due to the symmetric and antisymmetric vibrations, and the ν_4 band of CH$_4$ at ~7.7 μm (1300 cm^{-1}). The absorption coefficients for these bands were taken from Hudgins et al.[15] For our samples at low temperatures we used $A = 8.085 \times 10^{-18}$ cm/molecule for pure CH$_4$ ice (corrected assuming a CH$_4$ density of 0.47 g cm^{-3}), and $A = 2.43 \times 10^{-16}$ cm/molecule for water (corrected assuming a H$_2$O density of 0.7 g cm^{-3}). A small temperature correction[15] was applied in mixtures at 40 and

60 K yielding 8.17×10^{-18} cm/molecule for CH$_4$, and 2.53×10^{-16} cm/molecule for water.

As mentioned above, the film thickness, d, of the pure species is derived by simulating our transmission spectra with the adequate optical constants taken from the literature.[15] The same procedure is used to estimate the thickness of the ASW samples used for sequential deposition. For simultaneously deposited ice mixtures the determination of film thickness is more complicated and only a rough estimate can be given. We have used the following expression:

$$d = \frac{N_{\text{H}_2\text{O}} + N_{\text{CH}_4}}{\rho} \qquad (2)$$

where $N_{\text{H}_2\text{O}}$ and N_{CH_4} are the column densities of water and methane, respectively, and ρ is the density of the ice mixture. This density of the mixture is unknown, in principle, but it can be conjectured that for vapor deposited ices from a diffuse background gas at 14 K, it will lie between the values of pure H$_2$O and pure CH$_4$ deposited under the same conditions. For a given molecular ratio, we have taken the corresponding average density. Note that the range of densities contemplated is not too large (between ~0.5 g cm^{-3} for CH$_4$ and 0.7 g cm^{-3} for H$_2$O). The estimated uncertainties in the d values for mixtures are in the 20–30% range. It should be stressed at this point that an accurate knowledge of the film thickness is not crucial for the objectives of the present work.

3. Spectroscopic results and discussion

Fig. 1 presents an overview of spectra of a CH$_4$/H$_2$O = 0.4 co-deposited sample at 14 K and after warming at 60 K. Spectra of the pure components are well known and are not reproduced here. They can be seen for instance in Gálvez et al.[19] We discuss in this section the most relevant spectral features specific for the mixtures, namely the methane ν_1 band and the water dangling bond bands.

3.1 The CH$_4$ ν_1 band

One of the most striking findings in this investigation is the observation of the ν_1 band of CH$_4$, corresponding to the breathing vibration, which is forbidden by symmetry in the
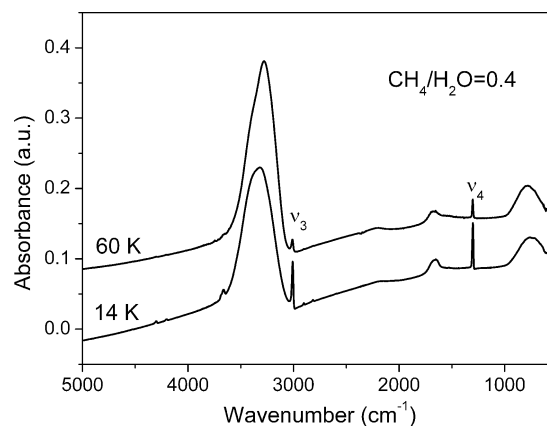

Fig. 1 IR spectrum of a CH$_4$/H$_2$O = 0.4 co-deposited ice mixture at 14 K and heated at 60 K. The estimated film thickness is 160 (±40) nm. Spectra are offset for clarity.

This journal is © the Owner Societies 2010

Phys. Chem. Chem. Phys., 2010, **12**, 3164–3170 | 3165

infrared spectra of gas phase and in pure CH_4 crystals. It is present in all our spectra of CH_4/H_2O mixtures, at ~ 2904 cm^{-1}, and its spectroscopic behaviour can be used to derive information on the type of H_2O–CH_4 association and interaction. Fig. 2 shows enlarged views of the 2750–2950 cm^{-1} spectral region of both simultaneously and sequentially deposited samples, illustrating also their temperature variation. The samples were formed by deposition at 14 K and later warmed up to 60 K. The spectra reveal different behaviour of this band depending on the formation process, which can be better appreciated by comparison to the symmetry-allowed $\nu_1 + \nu_4$ combination band. In simultaneous deposition experiments (upper panel), the ν_1 band is weak but noticeable from the beginning of the deposition at 14 K, and its relative intensity with respect to $\nu_1 + \nu_4$ does not change in the warming process until 60 K, where most of the CH_4 is already evaporated. At this temperature some methane fraction must remain as the strongest CH_4 vibrations, and traces of ν_1, are still seen. On the other hand, in sequential deposition experiments, the ν_1 band is extremely weak initially, becomes stronger at 30 K, always with respect to the combination band, and then again a trace only is left at 60 K. A possible explanation of these facts is proposed below, after the results on the dangling bonds are presented.

3.2 The H_2O dangling bond bands

Dangling bonds in solid water give rise to two bands (DB1 and DB2, at 3720 and 3696 cm^{-1} respectively) attributed to OH vibrations of doubly- or triply-coordinated surface molecules, and have been related to the porosity of the sample (see *e.g.* ref. 23 and 30). Their intensity relative to the fundamental vibrational bands of water rises with increasing surface to
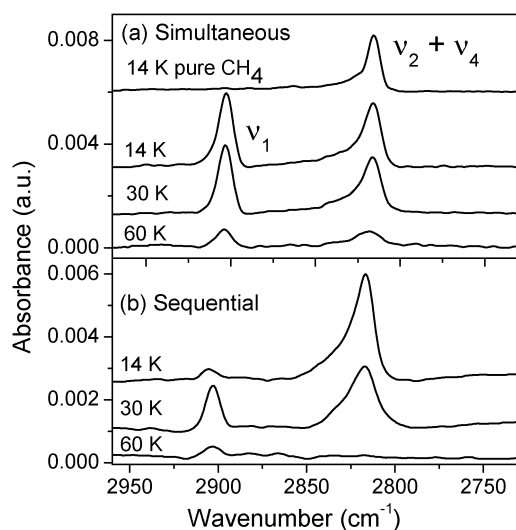

Fig. 2 IR spectra in the 2750–2950 cm^{-1} region. (a) CH_4/H_2O = 0.4 simultaneously deposited ice mixture at 14 K and warmed afterwards to the indicated temperatures; the spectrum of a pure methane ice is also included for comparison. (b) CH_4/H_2O sequential sample generated at 14 K and warmed to 30 and 60 K. Spectra are offset for clarity. A film thickness of 180 ($\pm$40) nm has been estimated for the simultaneously deposited sample in panel (a) and of 330 ($\pm$30) nm for the sequential sample of panel (b). The pure methane ice film is 80 ($\pm$10) nm thick.

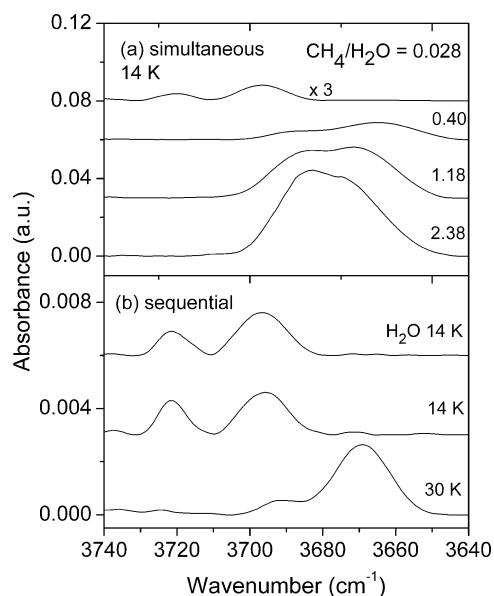**Fig. 3** Detail of the dangling bonds spectral IR region. (a) CH_4/H_2O simultaneously deposited samples generated at 14 K at varying molecular abundance ratios in the solid. The estimated film thicknesses are 360, 180, 330 and 460 nm, from top to bottom with uncertainties in the 20–30% range. (b) Sequential sample generated at 14 K and heated to 30 K. A pure water spectrum is also presented for comparison (upper trace). Both samples are 250 nm thick with 10% uncertainty.

volume proportion in the ice. Our experiments have detected spectral variations for these bands in CH_4/H_2O mixtures, and again different behaviour is observed associated to the kind of deposition scheme. Fig. 3 presents spectra in the 3640–3740 cm^{-1} region. The upper panel presents spectra of simultaneously deposited samples with roughly the same amount of water molecules, except for the top spectrum which has twice the water content for a better appreciation of the weak DB signals. When the sample is formed by co-deposition of the vapours at 14 K (upper panel), the DB1 and DB2 bands are not altered for very low CH_4 proportion, but when the methane concentration is increased, the bands are red-shifted and their intensity grows markedly. In sequentially deposited mixtures, the DB1 and DB2 bands are not altered by the admission of methane at 14 K. However, when the sample is warmed at 30 K, a red-shift of these bands is observed, as in the co-deposition experiment.

3.3 Discussion

In the following interpretation of the spectroscopic results we will make implicit use of information gathered from the adsorption isotherm analysis presented below. The main conclusion of such analysis concerns the microporous structure of AWS ices at 14 K.

The ν_1 band of methane is a strong feature in Raman spectra, either of the gas phase[31] or from noble gas matrices,[32] and has recently been reported in infrared spectra of CH_4 ice mixtures by Hodyss *et al.*[20] and Gálvez *et al.*[19] The observation of this breathing vibration in infrared spectra implies a breakdown of the symmetry of the system, and consequently the formation of a distorted form of CH_4. The adsorption of

3166 | *Phys. Chem. Chem. Phys.,* 2010, **12**, 3164–3170

This journal is © the Owner Societies 2010

CH$_4$ molecules on water ice surfaces, or the presence of very small methane crystallites distorted from their cubic structure through interactions with the amorphous water environment, could cause such an effect. This result bears some similarity to the observation of a distorted form of CO$_2$ in ice mixtures with water[25,33,34] or methanol.[35] In the CO$_2$ case, the distorted CO$_2$ structure gave rise to band shifts of several wavenumbers with respect to the bands of pure or undistorted CO$_2$, which was also present in the mixtures. For methane the interaction with water seems weaker, and CH$_4$-dist, as we may call this distorted structure, is mainly manifested by the appearance of the forbidden ν_1 band. Small shifts or broadenings are also observed on some of the other bands,[19] but they do not allow an independent and simultaneous identification of both methane structures.

To achieve a better understanding of this problem, we performed series of measurements varying the CH$_4$/H$_2$O concentration ratio and also the sample temperature. Fig. 4 summarizes some of our results for mixtures formed in simultaneous deposition experiments. The upper panel shows the increase in the absolute intensity of the "forbidden" ν_1 band of CH$_4$ with increasing methane concentration, for mixtures co-deposited at 14 and 40 K. The next graph presents an interesting magnitude, the measured intensity ratio between this ν_1 band and the strong fundamental CH$_4$ ν_4 band. The forbidden ν_1 band is due to CH$_4$-dist only, whereas ν_4 contains contributions from both distorted and normal methane, and therefore this quotient gives some idea of the relative amount of CH$_4$-dist in the sample. The graph shows that this ratio grows very quickly at 14 K for small values of the CH$_4$/H$_2$O concentration, reaches a maximum at CH$_4$/H$_2$O ratios of about 0.4 and then drops. The data measured at 40 K indicate a parallel drop in the distorted to normal methane ratio, occurring at lower methane to water concentrations. In the pure CH$_4$ limit, with no interaction with water to cause the distortion, CH$_4$-dist should not exist. On the other hand, the intensity of DB bands, displayed in the lower graph of Fig. 4, indicates that these bands become stronger with increasing CH$_4$ concentration. Our interpretation of these phenomena is the following. When methane and water are admitted simultaneously into the chamber, they mix intimately providing distorted environments that favour the appearance of CH$_4$-dist. When methane is added in higher concentrations, it tends to form larger "islands" where the CH$_4$-dist relative concentration is smaller, but where the surface in contact with amorphous water ice, responsible for the DBs, is also higher.

Fig. 4 depicts also the same magnitudes after heating the samples to 60 K. At that temperature, most of the methane has sublimated, but a small, constant fraction remains. This fraction probably corresponds basically to CH$_4$-dist in the inner recesses of the bulk ASW, keeping the same value that it had for the lowest CH$_4$/H$_2$O proportions. In a recent work,[19] the amount of methane retained in co-deposited samples heated at 60 K was estimated to have a saturation value of $\sim 10 \pm 2\%$ irrespective of the initial CH$_4$ excess concentration. In the former investigations on CO$_2$/H$_2$O and CO$_2$/CH$_3$OH mixtures mentioned above,[25,33–35] some CO$_2$ was also retained above its sublimation temperature, ~ 90 K.
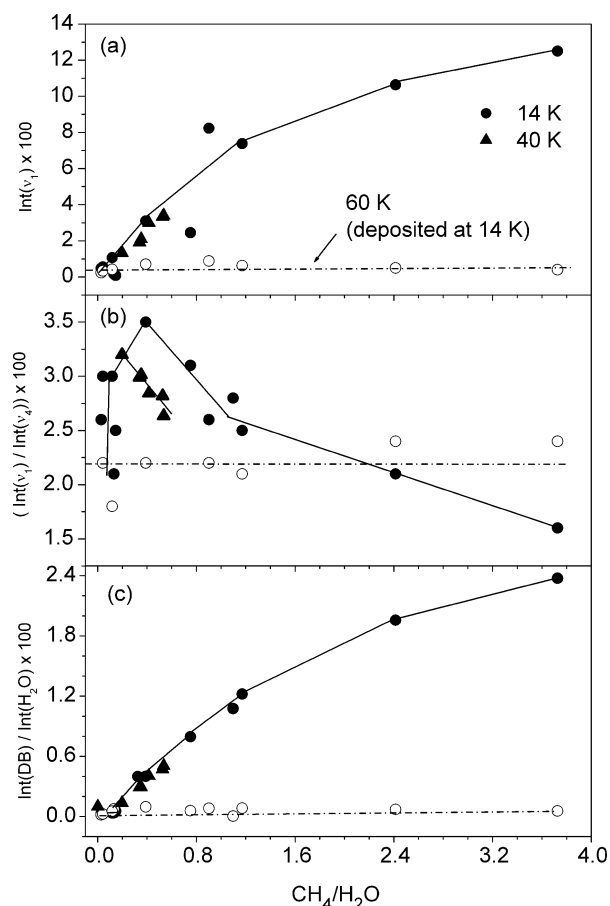

Fig. 4 (a) Integrated intensity of the "forbidden" ν_1 band of methane *versus* CH$_4$/H$_2$O molecular ratio for co-deposited samples. Solid circles: ice films generated at 14 K; triangles: deposition at 40 K; open circles: samples deposited at 14 K and heated to 60 K. (b) Methane ν_1/ν_4 integrated band intensity ratio from the same experiments. (c) Intensity ratio of DB bands with respect to the OH stretching band of water from the same experiments. All symbols as in previous panels.

When ASW is formed first, addition of methane at 14 K results in the growth of a CH$_4$ layer adsorbed on the external surface of the ice, with a minimum interaction with water, characterized by a very weak ν_1 band of CH$_4$-dist, and no change in the DB spectral bands as compared to water ice. However, if the sample is heated to 30 K, some fraction of methane molecules enter the ice and become adsorbed in narrow channels or micropores, either due to a higher CH$_4$ diffusion rate at that temperature or because of changes taking place in the structure of ASW. This part of the methane concentration is in the CH$_4$-dist form, with a visible ν_1 band. Further heating to 60 K induces sublimation of most CH$_4$, but, as for co-deposited samples, a small amount is retained, showing a weak but non-null ν_1 band and no trace of $\nu_2 + \nu_4$. The results from both experimental methods confirm the existence of a distorted form of CH$_4$, kept in narrow and internal cavities of ASW, where it can stay above the sublimation temperature of methane. Note that the micropore size currently estimated for this type of ASW samples does not exceed three CH$_4$ molecular diameters,[23] which implies a very close interaction between CH$_4$ and the surrounding H$_2$O environment.

Fig. 5 presents the results of a study on the dependence of these effects on the thickness of the ASW formed prior to CH_4 addition. The figure represents the CH_4/H_2O intensity ratio for the CH_4 ν_1 band (solid circles) and the CH_4 ν_4 band (open circles), for ices formed at 14 K and warmed to 30 and 60 K, respectively. The CH_4 ν_4 band is chosen at the higher temperature because ν_1 is too weak to allow intensity measurements to be performed. Both intensity ratios decrease with growing thickness of the ASW layer, indicating that the CH_4 introduced into the ice must occupy internal positions close to the surface, and is not evenly distributed into the bulk, which would yield constant growth with the ice thickness. Raut *et al.*[23] reported similar results for CH_4 adsorption experiments carried out at 40 K. Making use of the integrated intensity data mentioned above, it is possible to estimate from the values represented in Fig. 5 the relative amount of distorted methane retained in sequentially deposited samples. This value depends on the water ice film thickness. At 60 K, it varies from 1.6% for the thicker ASW films studied (400 nm) to 2.3% for the thinner ones (80 nm). We believe that in these thin films we are close to the limit of total diffusion of methane. In consequence, approximately four times more methane is retained at 60 K when the sample is generated by simultaneous deposition than in sequential experiments. This result is in accordance with intuitive expectations that the trapping of methane in the bulk of the ice or in inner cavities should be more efficient in co-deposited samples.

4. Adsorption isotherms

Information about the morphology of the ASW samples and about the desorption energy of CH_4 from the ice surface can be derived from adsorption isotherms. The upper panel of Fig. 6 shows the results for adsorption of CH_4 on ASW at 40 and 50 K. The two amorphous ice samples had the same thickness ($\sim$195 nm). In the figure, the molecular ratio of adsorbed methane to ASW, given by the respective integrated band intensities, is represented as a function of the equilibrium methane pressure normalized by the corresponding saturation
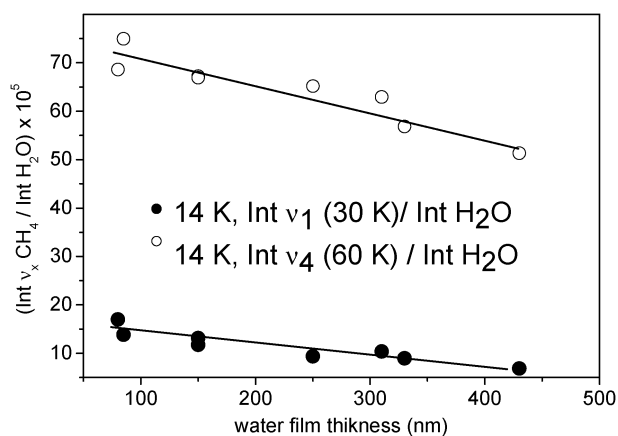

Fig. 5 Solid circles: integrated ν_1 CH_4/OH stretching H_2O band intensity ratio *versus* water ice film thickness for ices generated at 14 K and heated to 30 K. Open circles: integrated ν_4 CH_4/OH stretching H_2O band intensity ratio *versus* water ice film thickness for the same samples heated to 60 K.
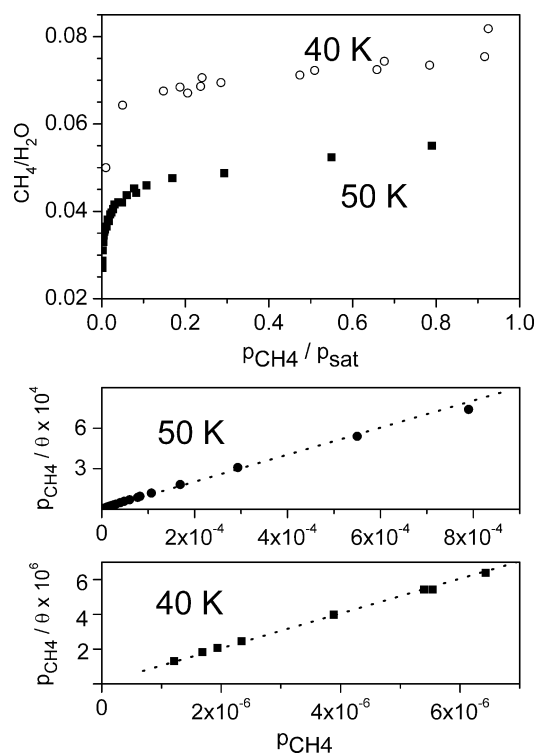

Fig. 6 Upper panel: CH_4/H_2O molecular ratio for sequential ice mixtures generated at 40 K and 50 K, *versus* the relative methane pressure ratio used for its generation. The water ice film thickness was 195 nm for both temperatures. The saturation pressures were 8.2×10^{-6} mbar and 1.0×10^{-3} mbar for 40 and 50 K respectively. Lower panels: fit of the data from the upper panel to Langmuir isotherms (eqn (5) in the text).

pressure. The resulting isotherms are of type I,[36,37] with a roughly flat plateau characteristic of microporous solids as expected for ASW at this temperature (see ref. 38 and references therein). The amount of adsorbed methane decreases with growing temperature, indicating that the ASW becomes less porous when it is formed at higher temperatures. Horimoto and coworkers[22] studied methane absorption on D_2O ices grown at 25 K and annealed at different temperatures. They conclude that up to 80 K the microporous structure of ices generated at 25 K is not affected by the heating. Our observations show that the temperature of generation of the ASW samples affects the microporous structure more drastically than the annealing process.

The data of Fig. 6 can be fitted to type I Langmuir isotherms:

$$\theta = \frac{x}{x_m} = \frac{bp}{1+bp} \qquad (3)$$

where θ is the surface coverage, *i.e.* the fraction of a monolayer actually occupied by adsorbed molecules, and b is the adsorption coefficient given by:

$$b = K \exp (E_d/RT) \qquad (4)$$

where K is a constant and E_d the desorption energy. Eqn (3) can be expressed as:

$$\frac{p}{\theta} = \frac{1}{b} + p = C + p \qquad (5)$$

In the two lower panels of Fig. 6, the measured data have been represented as (p/θ) *vs.* p. The surface coverage, θ, for each CH_4/H_2O value has been estimated by assuming that unit coverage is attained at p_{sat}. A fit of the data to straight lines with unit slope (eqn (5)) allows the determination of the adsorption coefficient, which is the inverse of the intercept, C. Combining the data from 40 and 50 K and using eqn (4) a desorption energy $E_d = 0.074 \pm 0.010$ eV is obtained. The use of the Langmuir isotherm for the derivation of E_d assumes tacitly that the adsorption energy is independent of site or surface coverage. A more elaborate treatment based on the isotherms of Freundlich[37] and Dubinin-Astakhov[39] for micro-porous solids was employed by Raut *et al.*[23] for the analysis of their data on the 40 K adsorption of CH_4 deposited on ASW from collimated vapour sources at various incidence angles. The most probable binding energies for methane adsorption reported by these authors range from 0.083 to 0.077 eV depending on the incidence angle. These values are in good agreement with the desorption energy determined in the present work.

In their studies about the adsorption of different gases on ices of astrophysical interest, Sandford and Allamandola[40] used the "sticking zero" condition of the gas on the surface for the estimate of desorption energies. This method, which has been used in previous works of our group,[33,35] assumes that deposition ceases when the average residence time of the molecules on the surface is equal to the time during which the ice surface is hit by a number of molecules equivalent to one monolayer coverage, t_m. For a given ice temperature, the "sticking zero" condition describes the equilibrium situation between the gas and the ASW at the limit of p_{sat}. The desorption energy is estimated with the expression:[28,33]

$$E_d = RT \ln (\nu_0 t_m) \tag{6}$$

where ν_0 is the frequency of oscillation of the molecules on the surface and t_m is given by.

$$t_m = n_s/(1/4)n\langle v\rangle \tag{7}$$

where n_s is the monolayer surface density; n, the molecular density for a given pressure and $\langle v\rangle$ the average molecular velocity at the corresponding gas temperature. To apply this procedure, the effective mean CH_4 molecular area and the frequency of oscillation of the adsorbed CH_4 molecules on the surface, ν_0, are required. We have taken a molecular area of 14.77 $Å^2$ from the CH_4 ice density given by Satorre *et al.*[29] and $\nu_0 = 1.57 \times 10^{12}$ s^{-1} for CH_4 adsorbed on Cu(001) at 58 K as measured by Graham *et al.*[41] The energy values calculated with eqn (6) are 0.093 and 0.095 eV for data at 40 and 50 K, respectively. With these data we can give an estimate of the desorption energy, $E_d = 0.094 \pm 0.010$ eV, which provides an average desorption energy for the different adsorption sites available in the ASW. This result is somewhat higher than the $E_d = 0.074 \pm 0.01$ determined from the Langmuir isotherm and also than the binding energies reported by Raut and coworkers.[23]

It should be mentioned here that the collision frequency from gas kinetic theory used for the derivation of eqn (6) might not be accurate for micropores of very small diameter;

still this procedure provides a reasonable estimate of E_d. The energy of desorption of CH_4 molecules from water–ice is about three times lower that the corresponding value for CO_2.[28,33]

5. Summary and conclusions

This paper presents the results of an investigation on CH_4/H_2O ice mixtures at cold temperatures by means of infrared spectroscopy, aiming to improve the present understanding of the interactions in these species. The main conclusions drawn from this work are summarized below.

Our samples were prepared by vapour deposition at temperatures of 14, 40 and 50 K, with CH_4/H_2O ratios ranging from 0.028 to 3.6. The deposited ice films were also heated up to 60 K to study their temperature evolution.

The appearance of the symmetry forbidden ν_1 band of methane in the solid samples is indicative of the presence of CH_4 molecules in a distorted environment within the ice. By comparison to similar but more marked effects encountered in CO_2/H_2O and CO_2/CH_3OH mixtures, we conclude that the distortions of the molecular environment must be caused by weak interactions.

Vapour deposited amorphous water ices in the 40–50 K temperature interval are microporous as demonstrated by the type I isotherms obtained for the adsorption of CH_4. The application of simple adsorption models leads to desorption energies in the ~ 0.074–0.094 eV range. These results are in agreement with recent literature estimates. The effective area for adsorption decreases appreciably when the deposition temperature grows from 40 to 50 K. This effect of deposition temperature is in contrast with that of annealing, which has recently been reported not to change the microporous structure of the sample over the temperature range considered.[22]

A joint analysis of the evolution of the water dangling bond bands and the ν_1 methane band shows that at 14 K methane deposited on amorphous water ice does not enter the micro-porous structure. At 30 K the methane molecules have enough mobility to diffuse inside the pores. ASW may have experienced a rearrangement of its structure that also facilities the methane mobility. The micropores, with an estimated size of less than three CH_4 molecular diameters, could provide the asymmetrical environment of close water–methane interaction responsible for the appearance of the forbidden ν_1 band. In contrast, when methane and water are admitted simulta-neously, distorted methane is formed from the lowest temperature, 14 K. Islands of solid CH_4 seem to form in the ice for CH_4/H_2O molecular ratios larger than 0.3.

Heating the ice samples to 60 K leads to evaporation of most of the methane, but a small fraction is retained, largely in the CH_4 distorted structure. This fraction is about four times larger in co-deposited mixtures than in the sequentially deposited samples.

Acknowledgements

References

1 M. H. Moore, R. L. Hudson and R. F. Ferrante, *Earth, Moon, Planets*, 2003, **92**, 291.

2 R. Hodyss, J. D. Goguen, P. V. Johnson, C. Campbell and I. Kanik, *Icarus*, 2008, **197**, 152.

3 D. A. Williams, W. A. Brown, S. D. Price, J. M. C. Rawlings and S. Viti, *Astronomy & Geophys.*, 2007, **48**, 25.

4 G. Notesco, D. Laufer and A. Bar-Nun, *Icarus*, 1997, **125**, 471.

5 A. C. A. Boogert, W. A. Schutte, A. G. G. M. Tielens, D. C. B. Whittet, F. P. Helmich, P. Ehrenfreund, P. R. Wesselius and T. de Graauw, *Astron. Astrophys.*, 1996, **315**, L377.

6 J. Licandro, N. Pinilla-Alonso, M. Pedani, E. Oliva, G. P. Tozzi and W. M. Grundy, *Astron. Astrophys.*, 2006, **445**, L35.

7 K. I. Öberg, A. C. A. Boogert, K. M. Pontoppidan, G. A. Blake, N. J. Evans, F. Lahuis and E. F. van Dishoeck, *Astrophys. J.*, 2008, **678**, 1032.

8 G. Zasowski, F. Kemper, D. M. Watson, E. Furlan, C. J. Bohac, C. Hull and J. D. Green, *Astrophys. J.*, 2009, **694**, 459.

9 T. C. Owen, H. Niemann, S. Atreya and M. Y. Zolotov, *Faraday Discuss.*, 2006, **133**, 387.

10 H. B. Niemann and the GCMS Team, *Nature*, 2005, **438**, 779.

11 M. Choukroun, G. Tobie and O. Grasset, *Lunar & Planet. Science XXXVII*, 2006, 1640.

12 R. Signorell and M. Jetzki, *Phys. Rev. Lett.*, 2007, **98**, 013401.

13 E. Dartois and D. Deboffle, *Astron. Astrophys.*, 2008, **490**, L19.

14 C. C. Wang, P. Zielke, O. F. Sigurbjörnsson, C. R. Viteri and R. Signorell, *J. Phys. Chem. A*, 2009, **113**(42), 11129.

15 D. M. Hudgins, S. A. Sandford, L. J. Allamandola and A. G. G. M. Tielens, *Astrophys. J. Suppl.*, 1993, **86**, 713.

16 A. C. A. Boogert, W. A. Schutte, F. P. Helmich, A. G. G. M. Tielens and D. H. Wooden, *Astron. Astrophys.*, 1997, **317**, 929.

17 O. Kerkhof, W. A. Schutte and P. Ehrenfreund, *Astron. Astrophys.*, 1999, **346**, 990.

18 M. P. Bernstein, D. P. Cruikshank and S. A. Sandford, *Icarus*, 2006, **181**, 302.

19 O. Gálvez, B. Maté, V. J. Herrero and R. Escribano, *Astrophys. J.*, 2009, **703**, 2101.

20 R. Hodyss, P. V. Johnson, J. V. Stern, J. D. Goguen and I. Kanik, *Icarus*, 2009, **200**, 338.

21 L. Chaix and F. Dominé, *J. Phys. Chem. B*, 1997, **101**, 6105.

22 N. Horimoto, H. S. Kato and M. Kawai, *J. Chem. Phys.*, 2002, **116**(11), 4375.

23 U. Raut, M. Famá, B. D. Teolis and R. A. Baragiola, *J. Chem. Phys.*, 2007, **127**, 204713.

24 E. Carrasco, J. M. Castillo, R. Escribano, V. J. Herrero, M. A. Moreno and J. Rodríguez, *Rev. Sci. Instrum.*, 2002, **73**, 3469.

25 O. Gálvez, B. Maté, V. J. Herrero and R. Escribano, *Icarus*, 2008, **197**, 599.

26 B. Maté, A. Medialdea, M. A. Moreno, R. Escribano and V. J. Herrero, *J. Phys. Chem. B*, 2003, **107**(40), 11098.

27 Z. Dohnálek, G. A. Kimmel, P. Ayotte, R. S. Smith and B. D. Kay, *J. Chem. Phys.*, 2003, **118**, 364.

28 S. A. Sandford and L. J. Allamandola, *Astrophys. J.*, 1990, **355**, 357.

29 M. A. Satorre, M. Domingo, C. Millán, R. Luna, R. Vilaplana and C. Santonja, *Planet. Space Sci.*, 2008, **56**(13), 1748.

30 V. Buch and J. P. Devlin, *J. Chem. Phys.*, 1991, **94**, 4091.

31 D. Bermejo, R. Escribano and J. M. Orza, *J. Mol. Spectrosc.*, 1977, **65**, 345.

32 M. Sagara and M. Ikezawa, *J. Phys. Soc. Jpn.*, 1983, **52**, 327.

33 O. Gálvez, I. K. Ortega, B. Maté, M. A. Moreno, B. Martín-Llorente, V. J. Herrero, R. Escribano and P. J. Gutiérrez, *Astron. Astrophys.*, 2007, **472**(2), 691.

34 B. Maté, O. Gálvez, B. Martín-Llorente, M. A. Moreno, V. J. Herrero, R. Escribano and E. Artacho, *J. Phys. Chem. A*, 2008, **112**(3), 457.

35 B. Maté, O. Gálvez, V. J. Herrero and R. Escribano, *Astrophys. J.*, 2009, **690**, 486.

36 F. Rouquerol, J. Rouquerol and K. Sign, *Adsorption by Powders & Porous Solids*, Academic Press, London, 1999.

37 W. Rudzinski and D. H. Everett, *Adsorption of Gases on Heterogeneous Surfaces*, Academic Press, 1992.

38 R. A. Baragiola, Microporous Amorphous Water Ice Thin Films Properties and Their Astronomical Implications, in *Water In Confined Geometries*, ed. J. P. Devlin and V. Buch, Springer, Berlin, 2003.

39 M. M. Dubinin and V. A. Astakhov, *Adv. Chem.*, 1971, **102**, 69.

40 S. A. Sandford and L. J. Allamandola, *Icarus*, 1990, **87**, 188.

41 A. P. Graham, M. F. Bertino, F. Hofmann, W. Silvestri and J. P. Toennies, *J. Chem. Phys.*, 1997, **106**(6), 2502.